Targeting Extracellular Collagen Assembly to Enhance Functional Recovery in Composite Neuromuscular Trauma

A. Fertala, PhD [1], J. Fertala , PhD[1], A. Stolfe [3], N. Guerriero [3], A. Zhou [4], P. Beredjiklian [5], A. Giakas, MD [1,2], M. L. Wang, MD, PhD [1,2], M. Rivlin, MD [1,2], P.K. Beredjiklian, MD [1,2]

[1]Thomas Jefferson University, Philadelphia, PA, [2]Rothman Institute of Orthopaedics, Philadelphia, PA; [3]Sidney Kimmel Medical College, Thomas Jefferson University, Philadelphia, PA; [4]Rutgers University, Piscataway, NJ; [5]Haverford College, Haverford Township, PA

Jefferson
Thomas Jefferson University
HOME OF SIDNEY KIMMEL MEDICAL COLLEGE

Abstract

- Severe extremity trauma in combat or civilian accidents frequently results in composite musculoskeletal injuries, involving simultaneous damage to muscles and peripheral nerves. A major barrier to optimal healing and functional recovery, often leading to permanent disability in wounded warriors, is the development of excessive, rigid scar tissue (fibrosis). Current clinical options to reduce scarring either lack specificity or carry high risks of collateral tissue damage.
- To address this, we investigated a recombinant anti-collagen antibody (**ACA**) engineered to block the extracellular assembly of scar tissue, thereby preventing physical blockades to recovery without interrupting the body's natural intracellular healing pathways.

Methods

- We simulated severe traumatic injury using a rabbit model featuring a crushed peripheral nerve and volumetric muscle loss, mimicking battlefield extremity wounds (Fig. 1).
- ACA was delivered locally to the injury sites via a thermoresponsive hydrogel. Over a 16-week period, we tracked functional rehabilitation by measuring muscle strength (dorsiflexion) and nerve signal recovery (compound muscle action potential).
- We also analyzed the architecture of the resulting scar tissue using polarized light microscopy and Fourier transform infrared (FTIR) spectroscopy.

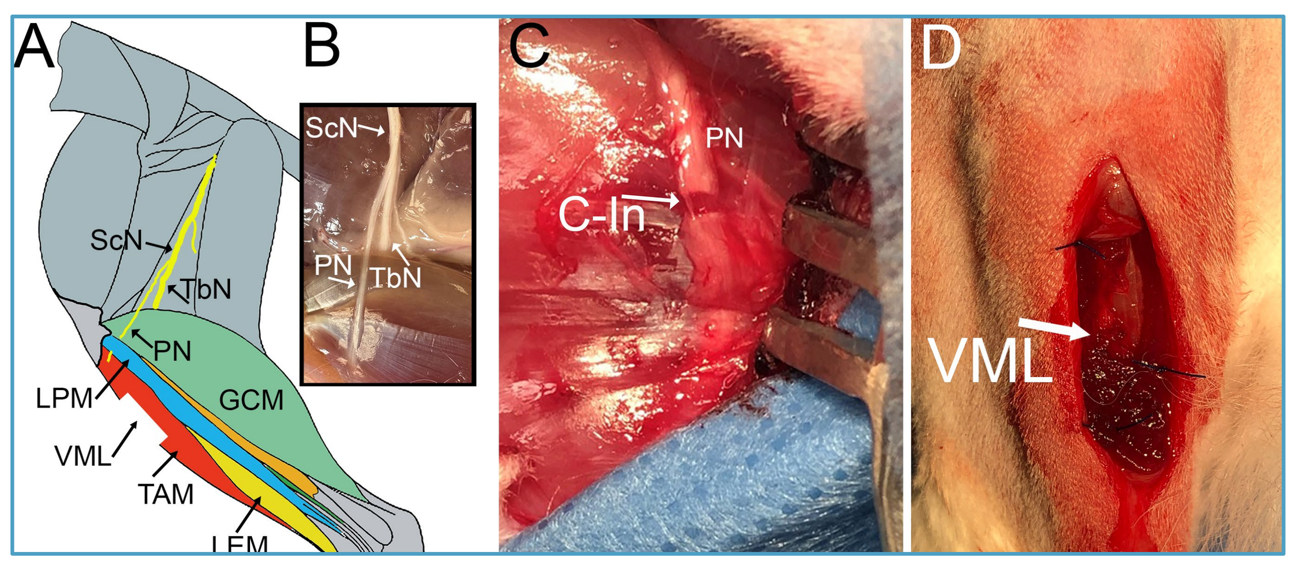

Figure 1. Anatomical location of the tibialis anterior muscle (TAM) and the peroneal nerve (PN) in the rabbit hind limb. (A) Schematic showing the anatomic position of TAM and PN targeted in this study. (B) The hind leg fragment showing the location of the PN. (C) Representative image of the crush injury site (C-In) in PN. (D) An image of the volumetric muscle loss (VML) injury. Abbreviations: GCM, gastrocnemius muscle; LEM, long extensor muscle; LMP, long peroneal muscle; PN, peroneal nerve; ScN, sciatic nerve; TAM, tibialis anterior muscle; TbN, tibial nerve; VML, volumetric muscle loss site.

Learning objectives

1. Describe how locally inhibiting extracellular scar formation can preserve tissue compliance and improve physical rehabilitation potential for traumatic combat wounds.
2. Analyze the functional strength recovery and structural scar modifications achieved by applying an anti-collagen antibody to severe muscle and nerve injuries.
3. Discuss the critical role of biological sex in post-traumatic scarring and how treatments must account for distinct fibrotic profiles to optimize veteran care.

Results

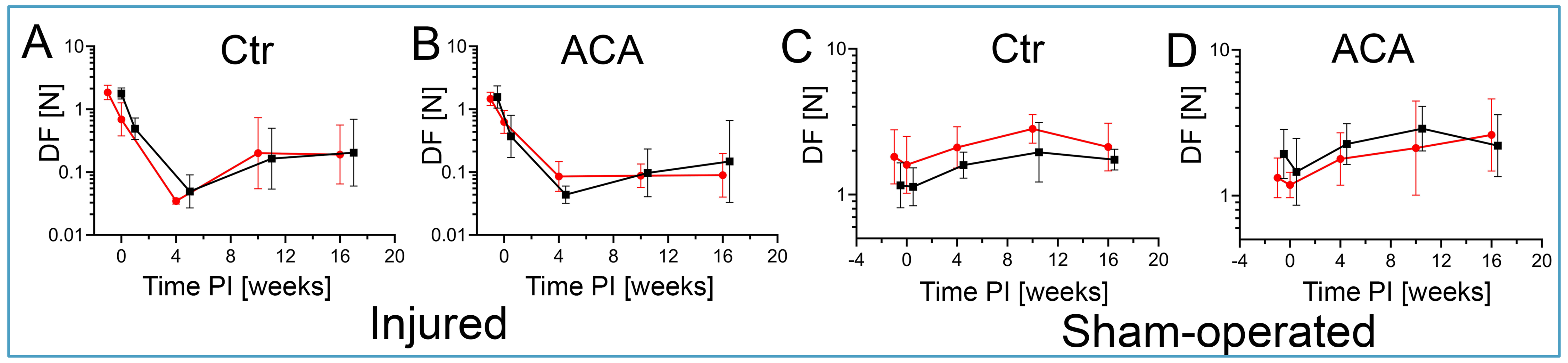

Figure 2. ACA treatment improves early dorsiflexion force (DF) recovery after composite injury, with sex-dependent effects. Graphic representation of longitudinal DF changes in the ACA-terated (ACA) and control (Ctr) groups. Each data point represents the geometric mean (GM) with its confidence interval (CI). Results indicate DF data for injured (A, B) and sham-operated (C, D) limbs. Red lines (●) represent female data, while black lines (■) depict male data. PI = post-injury

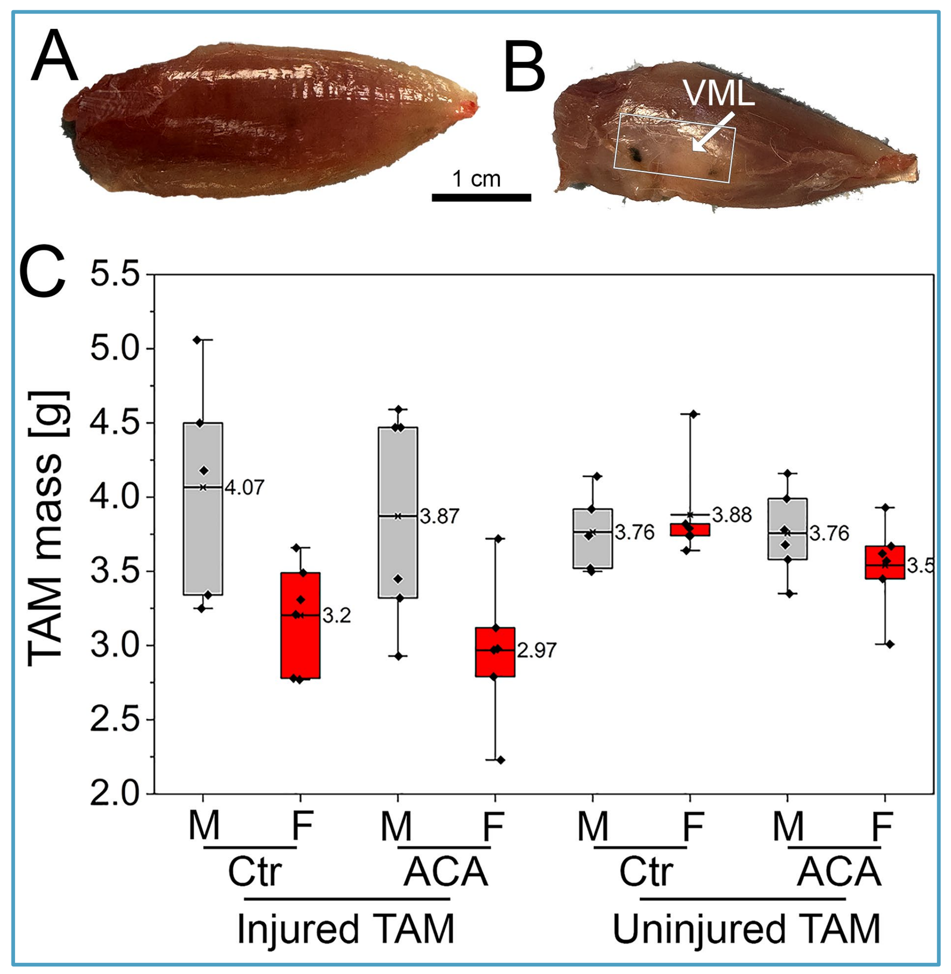

Figure 3. The tibialis anterior muscle (TAM) mass is differentially affected by injury in males and females.

(A) uninjured TAM, (B) injured TAM. In panel B, the approximate position of the volumetric muscle loss (VML) is indicated by the arrow and rectangle. (C) Graphic presentation of TAM's weights. Data are presented for males (M, gray boxes) and females (F, red boxes) from the control (Ctr) and ACA-terated (ACA) groups. Each box represents the interquartile range (25th to 75th percentile), the horizontal line within the box indicates the mean, and the whiskers represent the minimum-maximum range.

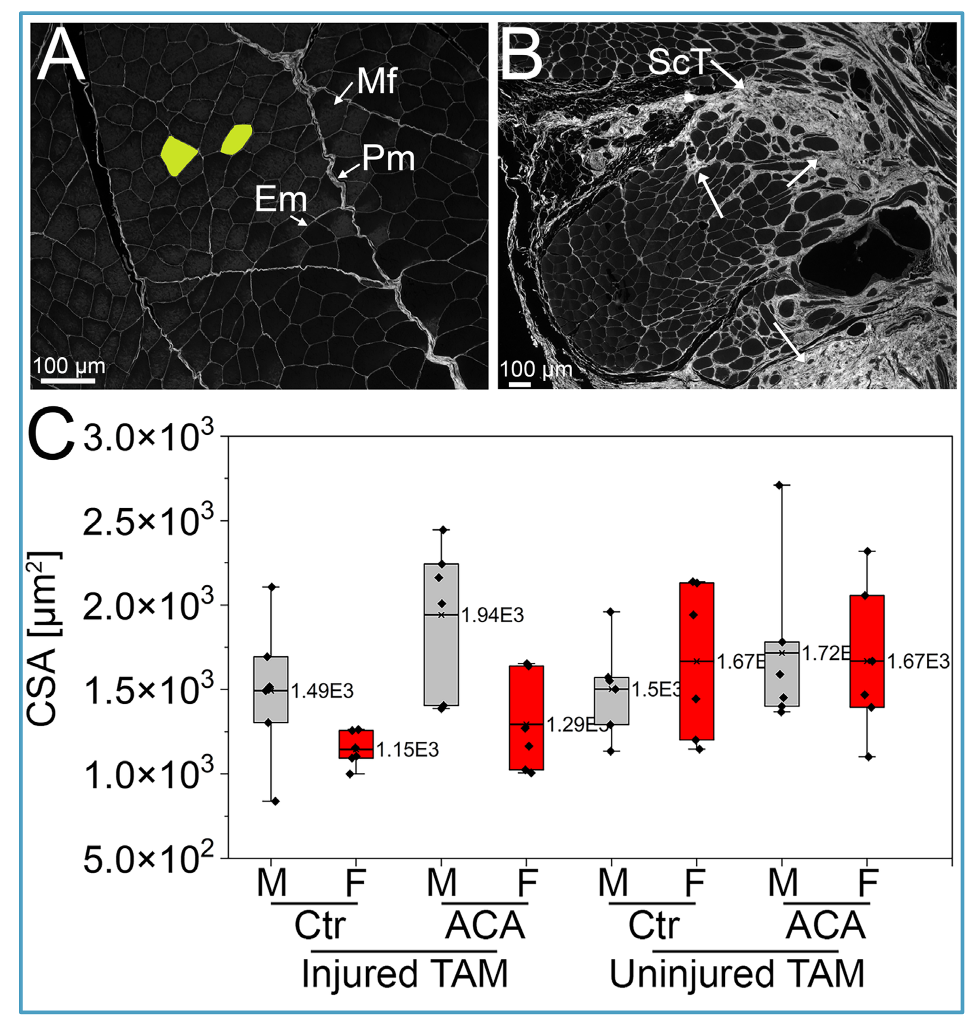

Figure 4. Injury and sex influence the cross-sectional area of tibialis anterior muscle (TAM) fibers. (A, B) Representative images of the cross-sections of uninjured (A) and injured (B) muscles. Samples were stained with picrosirius red and visualized using fluorescence microscopy to highlight endomysium boundaries. Representative cross-sectional areas (CSAs) are outlined to demonstrate how muscle fibers were defined for measurement. Using image analysis software, the CSAs delineated by the endomysium were quantified. Representative images show the muscles and corresponding sections from a female rabbit in the ACA-treated group. (C) Analysis of the CSAs from injured and uninjured limbs. Data are presented for males (M, gray boxes) and females (F, red boxes) from the control (Ctr) and ACA-treated (ACA) groups. Each box represents the interquartile range (25th to 75th percentile), the horizontal line within the box indicates the mean, and the whiskers represent the minimum-maximum range. Abbreviations: Em, endomysium; Mf, muscle fiber; Pm, perimysium; ScT, scar tissue.

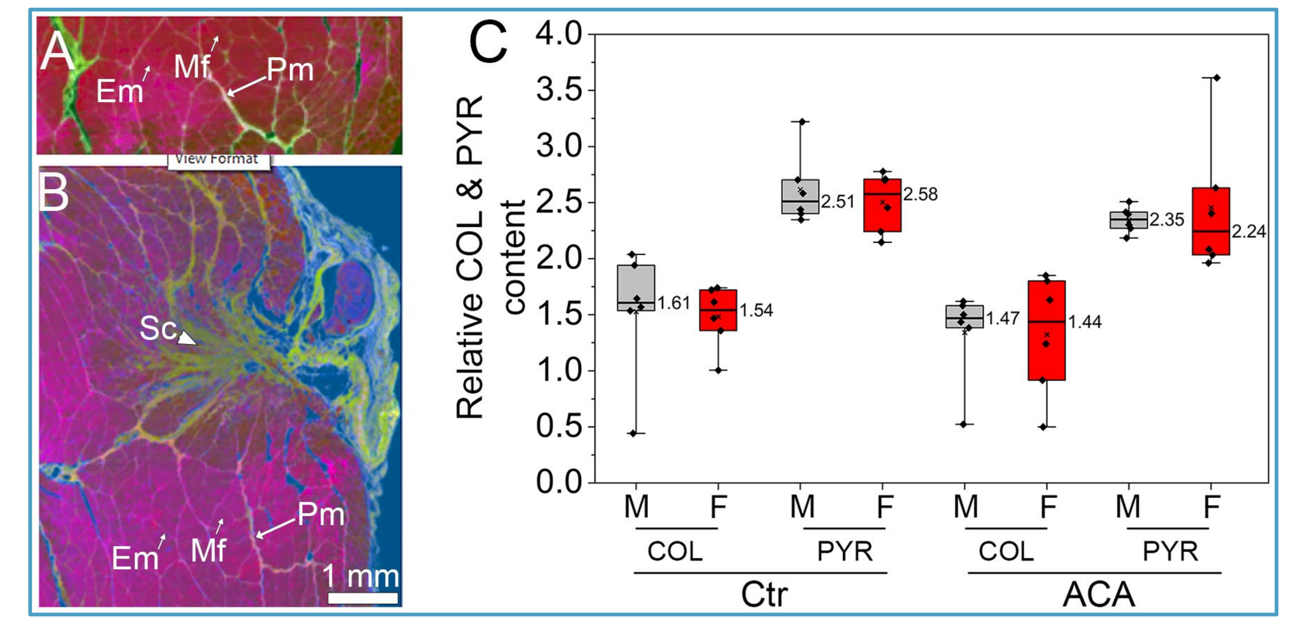

Figure 5. Fourier transform infrared (FTIR) spectroscopy imaging identifies collagen-rich scar regions in the injured tibialis anterior muscle (TAM) and points toward reduced collagen content and cross-link maturity in tibialis anterior scars. Representative images of unstained uninjured (A) and injured (B) TAMs. The images are pseudocolored based on FTIR spectroscopy-derived properties of the muscle regions. (C) FTIR spectroscopy data are presented for males (M, gray boxes) and females (F, red boxes) from the control (Ctr) and ACA-treated (ACA) groups. Each box represents the interquartile range (25th to 75th percentile), the horizontal line within the box indicates the median, and the whiskers represent the minimum-maximum range. Statistical significance was determined by using ANOVA on ranks, $p < 0.05$. Abbreviations: Em, endomysium; Mf, muscle fiber; Pm, perimysium; Sc, scar area. Representative images show muscle sections from a male rabbit in the ACA group.

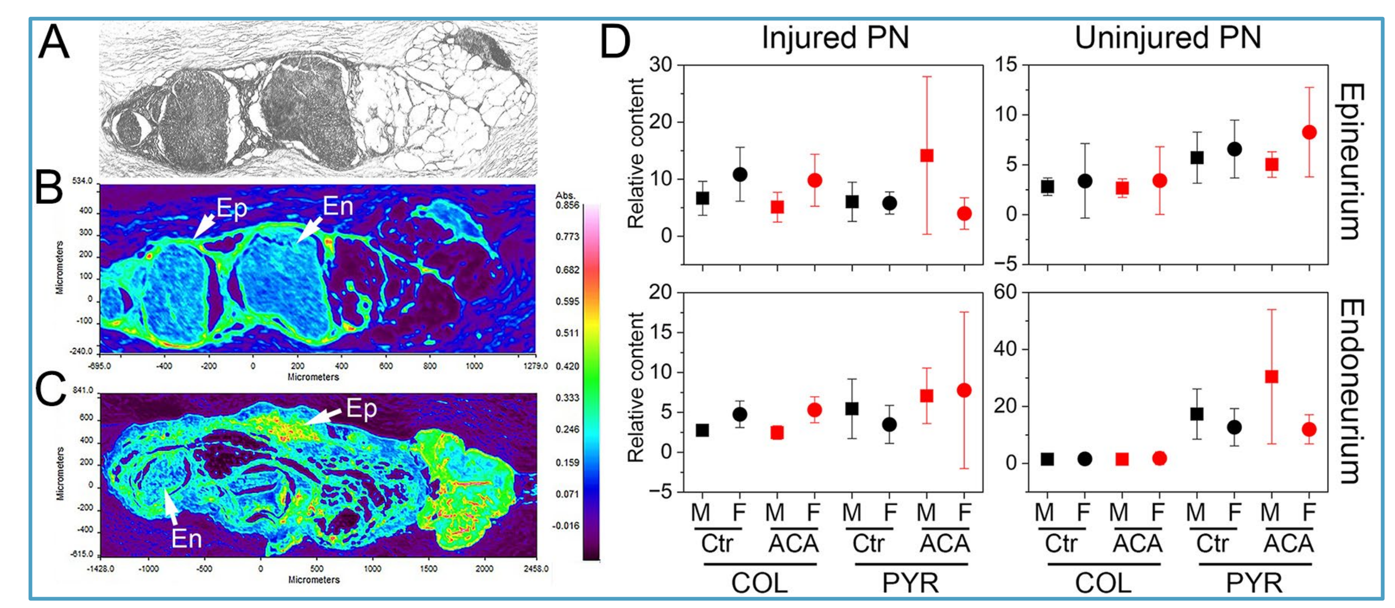

Figure 6. Peroneal nerve (PN) injury increases collagen (COL) content and alters pyridinoline (PYR) cross-links in epineurium and endoneurium. (A) Representative greyscale scan used to identify epineurial and endoneurial areas for Fourier transform infrared (FTIR) spectroscopy assays of collagen-rich deposits. Representative FTIR spectroscopy-based images of an uninjured nerve (B) and an injured nerve (C) are also presented. The scale bar indicates the relative absorbance of the analyzed areas. Epineuria (Ep) and endoneuria (En) are indicated by arrows. Representative images show PN sections from a female rabbit in the ACA-treated group. (D) FTIR spectroscopy-derived results are stratified by tissue layer (epineurium vs. endoneurium), injury status (injured vs. uninjured), and sex (M: male, square symbol ■; F: female, circle symbol ●) within the ACA-treated (ACA, red symbols) and control (Ctr, black symbols) groups. Each data point represents the geometric mean (GM) with its confidence interval (CI).

Conclusion

Locally intercepting scar formation with ACA represents a highly promising therapeutic strategy for composite trauma. By preserving muscle compliance and force early in the healing process, this treatment could vastly improve rehabilitation outcomes and mitigate permanent disability for wounded service members and veterans.